Chapter 2
General Analysis of Radar Sensors

2.1 Introduction

The operation and performance of radar sensors involve the propagation of electromagnetic (EM) waves (or signals as commonly referred to). The transmitter of a radar sensor transmits a signal toward a target or object. The signal, upon incident on the target, scatters in all directions due change of the electric and/or magnetic properties of the target relative to those of the medium surrounding the target, in which the signal is propagating. The scattered signals propagating in the direction of the receiving antenna are captured and processed by the receiver. Understanding the behavior of signals and analysis of scattered signals are hence important in order to understand the operation and performance of radar sensors as well as characterize the properties of targets, which are needed in the design and operation of radar sensors.

Two of the most important characteristics dictating the performance of radar sensors are "resolution" and "range" (or "penetration depth" as typically used in subsurface sensing). The angle or cross or lateral resolution depends on the antenna while the range resolution is determined by the absolute bandwidth of the signal or, specifically for stepped-frequency continuous-wave (SFCW) radar sensors, the width of the synthetic pulse corresponding to a target that a SFCW) system generates. These are discussed in details in Chap. 3. On the other hand, the range is determined by various parameters and is discussed in this chapter. Some of these parameters are determined by the designer and used in the design of the system and its constituent components such as transmitter's power, antenna gain, signal's frequency, and receiver's gain, noise figure, dynamic range and sensitivity. Some of these parameters are related. Other parameters are dependent upon the properties of the media, in which the signal propagates, and individual targets. The properties of the media directly affect the propagation constant involving the loss and velocity of the propagating signal, which essentially dictate how signal travels in the media.

C. Nguyen and J. Park, *Stepped-Frequency Radar Sensors*,
SpringerBriefs in Electrical and Computer Engineering,
DOI 10.1007/978-3-319-12271-7_2

Targets have their own properties and Radar Cross Section (RCS), and cause reflection, transmission, spreading loss, and scattering of incident signals. These parameters are not controlled by the designer. However, if known, they could provide valuable information to the design of the radar sensor's architecture and components and hence are important to the design of radar sensors.

This chapter addresses various topics concerning the analysis of radar sensors including signal propagation, which involves Maxwell's and wave equations, propagation constant; signal scattering from objects, which involves reflection, transmission, radar cross section; system equations including Friis transmission equation and radar equations in general and for half-space and buried targets; signal-to-noise ratio; receiver sensitivity; maximum range or penetration depth; and system performance factor.

2.2 Signal Propagation

The propagation of signals in a medium is governed by Maxwell's equations, or the resulting wave equations, and the medium's properties. These will be briefly covered in this section assuming steady-state sinusoidal time-varying signals.

2.2.1 Maxwell's Equations and Wave Equations

Maxwell's equations in differential (or point) form are

$$\nabla \times \vec{E} = -j\omega\vec{B} \tag{2.1a}$$

$$\nabla \times \vec{H} = \vec{J} + j\omega\vec{D} \tag{2.1b}$$

$$\nabla . \vec{D} = \rho \tag{2.1c}$$

$$\nabla . \vec{B} = 0 \tag{2.1d}$$

where $\vec{E}$, $\vec{H}$, $\vec{D}$, $\vec{B}$, $\vec{J}$, and ρ are the (phasor) electric field, magnetic field, electric flux density (or displacement field), magnetic flux density, current density, and volume charge density. They are functions of frequency and location.

The electric flux density, electric field intensity and the magnetic flux density, magnetic field intensity in a material are related by the following constitutive relations:

$$\vec{D} = \varepsilon_o \varepsilon_r \vec{E} = \varepsilon \vec{E} \tag{2.2}$$

and

$$\vec{B} = \mu_o \mu_r \vec{H} = \mu \vec{H} \tag{2.3}$$

where $\varepsilon_o = 8.854 \times 10^{-12}\,\mathrm{F/m}$ and $\mu_o = 4\pi \times 10^{-7}\,\mathrm{H/m}$ are the dielectric constant or permittivity and permeability of air, ε_r and ε are the relative dielectric constant (or relative permittivity) and dielectric constant (or permittivity) of material, respectively, and μ_r and μ are the relative permittivity and permittivity of material, respectively. Most materials are non-magnetic having μ_r close to 1. Also, most materials are "simple" media, which are linear, homogeneous, and isotropic having constant ε_r and μ_r.

The (conduction) current is related to the electric field by

$$\vec{J} = \sigma \vec{E} \tag{2.4}$$

where σ is the conductivity of material.

Although the electric and magnetic fields of signals in any medium, and hence signal propagation, can be determined from Maxwell's equations subject to boundary conditions, it is more convenient to determine them from (single) wave equations. The wave equations can be derived from Maxwell's equations as

$$\nabla^2 E - \gamma^2 E - j\omega\mu J - \frac{1}{\varepsilon}\nabla\rho = 0 \tag{2.5a}$$

$$\nabla^2 H - \gamma^2 H - \nabla \times J = 0 \tag{2.5b}$$

where $\gamma = \alpha + j\beta$ is the propagation constant with α (Np/m) and β (rad/m) being the attenuation and phase constant, respectively.

2.2.2 Propagation Constant, Loss and Velocity

In general, a medium is characterized by its complex dielectric constant or complex permittivity, which, in turn, results in a complex propagation constant for signals propagating in the medium. The real and imaginary parts of the propagation constant are known as the attenuation and phase constants and dictate the loss and velocity of signals, respectively. Practical media in which signals propagate are always lossy and dispersive, and hence are imperfect. Consequently, there is always loss present in any practical medium, known as dielectric loss, due to a non-zero conductivity of the medium. This loss reduces the transmitting power and hence the maximum range or penetration depth of a radar sensor. The velocity, on the other hand, determines the target's range.

The dielectric properties of a medium, including (practical) lossy and (ideal) lossless media, can be described by a complex dielectric constant or complex permittivity of the medium ε_c given as

$$\varepsilon_c \equiv \varepsilon' - j\varepsilon'' = \varepsilon - j\frac{\sigma}{\omega} \tag{2.6}$$

where

$$\begin{aligned} \varepsilon' &= \varepsilon = \varepsilon_o \varepsilon_r \\ \varepsilon'' &= \frac{\sigma}{\omega} \end{aligned} \tag{2.7}$$

Both ε' and ε'' are functions of frequency, and ε'' accounts for the loss in the medium. We can also characterize a lossy medium by its complex relative dielectric constant

$$\varepsilon_{cr} \equiv \frac{\varepsilon_c}{\varepsilon_o} = \varepsilon_r' - j\varepsilon_r'' = \varepsilon_r - j\frac{\sigma}{\omega\varepsilon_o} \tag{2.8}$$

Note that $\varepsilon_r' = \varepsilon_r$.

The loss in a medium is typically characterized in term of the loss tangent defined as the ratio between the imaginary and real parts of the complex dielectric constant:

$$\tan\delta \equiv \frac{\varepsilon''}{\varepsilon'} = \frac{\varepsilon_r''}{\varepsilon_r'} = \frac{\sigma}{\omega\varepsilon} = \frac{\sigma}{\omega\varepsilon_o\varepsilon_r} \tag{2.9}$$

which is of course dependent upon frequency. The loss tangent of a medium, just like its relative dielectric constant ε_r and complex relative dielectric constant ε_{cr}, can be measured.

The propagation constant of signals travelling in a lossy medium can be derived as

$$\begin{aligned} \gamma &= \alpha + j\beta = j\omega\sqrt{\mu\varepsilon_c} \\ &= j\omega\sqrt{\mu\varepsilon}\sqrt{1 - j\frac{\sigma}{\omega\varepsilon}} = j\omega\sqrt{\mu\varepsilon'}\sqrt{1 - j\frac{\varepsilon''}{\varepsilon'}} = j\omega\sqrt{\mu\varepsilon}\sqrt{1 - j\tan\delta} \end{aligned} \tag{2.10}$$

or

$$\gamma = jk_o\sqrt{\varepsilon_r' - j\varepsilon_r''} = jk_o\sqrt{\varepsilon_r'}\sqrt{1 - j\frac{\varepsilon_r''}{\varepsilon_r'}} \tag{2.11}$$

where $k_o = \omega\sqrt{\mu_o\varepsilon_o}$ is the wave number for air, considering non-magnetic medium having $\mu_r = 1$.

The velocity of a signal can be determined from the phase constant as

$$v = \frac{\omega}{\beta} \tag{2.12}$$

For media having small loss, $\sigma/\omega\varepsilon \ll 1$ or $\varepsilon_r'' \ll \varepsilon_r'$ and hence $\tan\delta \ll 1$, and the propagation constant in (2.10) and (2.11) can be approximated using the binomial series as

$$\gamma = \alpha + j\beta = \frac{k_o \varepsilon_r''}{2\sqrt{\varepsilon_r'}} + jk_o\sqrt{\varepsilon_r'} = \frac{\omega\sqrt{\mu_o\varepsilon'}}{2}\tan\delta + j\omega\sqrt{\mu_o\varepsilon'} \tag{2.13}$$

and the velocity is obtained as

$$v = \frac{1}{\sqrt{\mu_o\varepsilon_o\varepsilon_r}} = \frac{c}{\sqrt{\varepsilon_r}} \tag{2.14}$$

where $c = 3 \times 10^8$ m/s is the velocity in air.

For high-loss media, $\sigma \gg \omega\varepsilon'$ or $\tan\delta \gg 1$, we can obtain from (2.10) and (2.11):

$$\gamma = \alpha + j\beta = j\omega\sqrt{\mu\varepsilon}\sqrt{j\frac{\sigma}{\omega\varepsilon}} = \sqrt{j}\sqrt{\omega\mu\sigma} = (1+j)\sqrt{\pi f\mu\sigma} \tag{2.15}$$

and the velocity is given by

$$v = 2\sqrt{\frac{\pi f}{\mu_o\sigma}} \tag{2.16}$$

The developed microwave and millimeter-wave SFCW radar sensors to be presented in Chaps. 4 and 5 were used for some surface and subsurface sensing applications. One of the subsurface sensing measurements was done on pavement structures. A typical pavement consists of three layers: asphalt, base, and subgrade. The subgrade is basically natural soil of infinitely thick. The common pavement materials used in practice could be considered as low-loss and non-magnetic materials [30, 31]. Table 2.1 shows typical parameters of the asphalt and base [9]. The values of the real (ε_r') and imaginary (ε_r'') parts of the complex relative dielectric constant were measured at 3 GHz using a vector network analyzer based dielectric measurement system. These measurements were done over many samples in a laboratory setting.

Table 2.1 Typical electrical properties of pavement materials

Parameter	Asphalt	Base
ε_r'	5–7	8–12
ε_r''	0.035	0.2–0.8

The values of the parameters in Table 2.1 show that these pavement materials can be considered as low-loss materials. It is noted that these measurements were done in laboratory. In field environments, where a radar sensor is used for sensing, however, the situation is typically more complex, resulting in different material properties. The properties of these materials, characterized by their complex relative dielectric constants, are influenced significantly by environmental factors such as rain, snow, moisture, and temperature, etc. They are also a function of frequency, space in the structures, and the constituents of materials. In addition, the property of a given material may also vary substantially from one sample to another. These factors make the actual complex relative dielectric constants different from what measured in a laboratory and the actual materials could be very lossy.

Practical media such as pavement materials are dispersive, causing the phase constant β behave as a nonlinear function of frequency, which in turn results in frequency-dependent velocities as can be inferred from (2.12). As such, signals of different frequencies in a radar sensor travel with different velocities. The return signals from a target hence have different phases at different frequencies and the composite signal, after captured and combined by the receiver, becomes distorted. Consequently, the dispersion in materials and hence different velocities should be taken into account in the design of a radar sensor, especially when the operating frequency range is large and the frequencies are high. Also, at frequencies above 1 GHz, water relaxation effect becomes dominant [1], making the dispersion more pronounced.

The attenuation of a signal traveling in a medium is determined by the medium's properties. Considering this and the fact that the properties of (simple) media are independent of the waveform type and sources, we can assume that the signal is a sinusoidal uniform plane wave to simplify the formulation without loss of generality. To further simply the analysis, we assume that there is no charge ($\rho = 0$) and current ($\vec{J} = 0$) in the medium, and the signal propagates into the medium along the direction z and represent the signal using only the electric and magnetic field components along the x and y directions, respectively. The (phasor) electric and magnetic fields can be determined from wave equations (2.5a, b) as

$$\vec{E} = \vec{a}_x E_o \mathrm{e}^{-\alpha z} \mathrm{e}^{-j\beta z} \tag{2.17}$$

and

$$\vec{H} = \vec{a}_y H_o \mathrm{e}^{-\alpha z} \mathrm{e}^{-j\beta z} = \vec{a}_y \frac{E_o}{|\eta|} \mathrm{e}^{-\alpha z} \mathrm{e}^{-j\left(\beta z - \phi_\eta\right)} \tag{2.18}$$

where E_o and H_o are the initial magnitudes of the electric and magnetic fields (at $z = 0$), respectively, with $\eta = |\eta| \angle \phi_\eta$ being the intrinsic impedance of the medium. The magnitudes of the electric and magnetic fields hence reduce exponentially according to e^{-az} as the signal propagates in the z direction.

Equations (2.17) and (2.18) show that the amplitudes of the electric and magnetic fields are attenuated by

$$A = \mathrm{e}^{-\alpha d} \tag{2.19}$$

or, in dB,

$$A_{dB} = -20\alpha d \log e = -8.686\alpha d\ (dB) \tag{2.20}$$

over a distance d.

The time-average power density (W/m^2) of a signal is given as

$$\vec{S} = \frac{1}{2}\mathrm{Re}\left(\vec{E} \times \vec{H}^*\right) = \vec{a}_z \frac{E_o^2}{2|\eta|}\cos\left(\phi_\eta\right)\mathrm{e}^{-2\alpha z} \tag{2.21}$$

where (*) denotes the conjugate quantity. Equation (2.21) shows that power of a signal in a medium decreases exponentially at a rate of e^{-2az} as the signal travels in the direction of z. The total time-average power incident upon a surface S of a target can then be obtained as

$$\vec{P} = \frac{1}{2}\mathrm{Re}\int_S \left(\vec{E} \times \vec{H}^*\right) ds \tag{2.22}$$

Equations (2.21) and (2.22) allow the magnitude and direction of the real power of a signal travelling in any medium to be determined.

Some remarks need to be made here concerning the properties of materials involved in subsurface sensing and their general effects to the analysis and performance of a radar sensor. Subsurface media such as the asphalt and base materials of pavements are very complex. They are highly inhomogeneous, dispersive, and lossy. The inhomogeneity produces irregularities, which result in scattering and excessive high clutter noise, thus complicating the target detection. The dispersion distorts the return signal, and the high attenuation reduces and further distorts the return signal. As mentioned earlier, the properties of these materials are a function of frequency, space in the structures, material's constituents, and environmental factors. Furthermore, there is typically a close proximity between antennas and the ground encountered in the use of a radar sensor, and this complicates the radar signal's behavior. It is therefore very difficult, if not impossible, to analyze precisely the radar sensor's signal propagation in subsurface media existing in real testing environments. Consequently, this prevents an accurate calculation of the total loss of the signal as it propagates through the subsurface media and returns to the sensor.

2.3 Scattering of Signals Incident on Targets

Signals incident on a target are scattered and a portion of the scattered energy traveling toward the receiving antenna is captured by the antenna. In a given propagating medium, the scattering power is determined by the electromagnetic properties and physical structure of a target. As such, the power arriving to the receiving antenna can be estimated if the properties and structure of the target and propagating medium are known.

2.3.1 Scattering of Signals on a Half-Space

If a signal is incident on an interface between different media, part of its energy is reflected and part is transmitted through the interface. For simplicity, we assume the signal is a uniform plane wave. In the case of a flat surface, the reflection and transmission coefficients depend upon the polarization of the incident signal, the angles of incidence and transmission, and the intrinsic impedances of the media. There are two kinds of polarization: parallel and perpendicular polarizations. If the electric field is in the incident plane, the signal has a parallel polarization. Under the parallel polarization, and the magnetic field is perpendicular to the incident plane. Alternately, if the electric field is normal to the incident plane, the signal is in the perpendicular polarization and the magnetic field lies in the incident plane. Figure 2.1 illustrates the electric and magnetic fields for the parallel polarization.

2.3.1.1 Reflection at a Single Interface

Consider a single interface between two different media as shown in Fig. 2.1, by applying the boundary conditions for the tangential components of the electric and magnetic fields at the interface, we can derive the reflection (Γ_{par} and Γ_{per}) and transmission coefficients (T_{par} and T_{per}) for the parallel (par) and perpendicular (per) polarizations as

$$\Gamma_{par} = \frac{\eta_2 \cos\phi_t - \eta_1 \cos\phi_i}{\eta_2 \cos\phi_t + \eta_1 \cos\phi_i} \tag{2.23}$$

$$\Gamma_{per} = \frac{\eta_2 \cos\phi_i - \eta_1 \cos\phi_t}{\eta_2 \cos\phi_i + \eta_1 \cos\phi_t} \tag{2.24}$$

$$\mathrm{T}_{par} = \frac{2\eta_2 \cos\phi_i}{\eta_2 \cos\phi_t + \eta_1 \cos\phi_i} \tag{2.25}$$

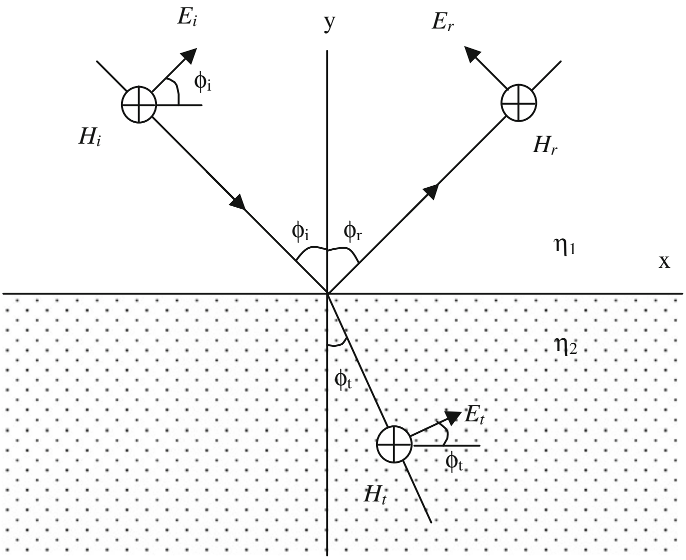

Fig. 2.1 Electric and magnetic fields of signals incident upon the interface between two different media for parallel polarization. The incident plane is *xy* plane

$$\mathrm{T}_{per} = \frac{2\eta_2 \cos\phi_i}{\eta_2 \cos\phi_i + \eta_1 \cos\phi_t} \tag{2.26}$$

respectively, where η_1 and η_2 are the intrinsic impedances of media 1 and 2, respectively, and ϕ_i and ϕ_t are the incident and transmitted angles, respectively. These angles are related by

$$\frac{\sin\phi_i}{\sin\phi_t} = \frac{\sqrt{\varepsilon_{r2}}}{\sqrt{\varepsilon_{r1}}} \tag{2.27}$$

where ε_{r1} and ε_{r2} are the relative dielectric constants of media 1 and 2, respectively. reflection and transmission coefficients are complex due to the fact that the intrinsic impedances are complex for (practical) lossy media.

Consider a parallel-polarized signal is incident on the interface through a lossy medium 1, as shown in Fig. 2.2, the time-average power density $S_r(R)$ reflected from the interface at the distance R from the interface can be found from (2.21) as

$$S_r(R) = \left|\Gamma_{par}\right|^2 \exp(-4\alpha_1 R) S_i(R) \tag{2.28}$$

where $S_i(R)$ is the average incident time-power density at R and α_1 is the attenuation constant of medium 1. The reflected power, which could be captured by the receiving antenna, is reduced due to the reflection at the interface and the attenuation in the propagating medium.

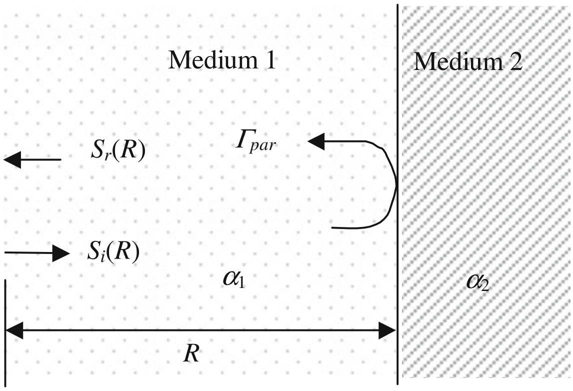

Fig. 2.2 Incident and reflected power away from an interface

Figure 2.3 shows the magnitudes of the reflection coefficients versus incident angle for both the parallel and the perpendicular polarizations of a plane wave incident on a flat surface between air and a lossless medium having relative dielectric constant of 2, 4, 6, 8 and 10.

The phase of the reflected signal from an interface at a particular location, relative to that of the incident signal, is determined by the phase of the reflection coefficient, the velocity in the propagating medium, and the distance of the location from the interface.

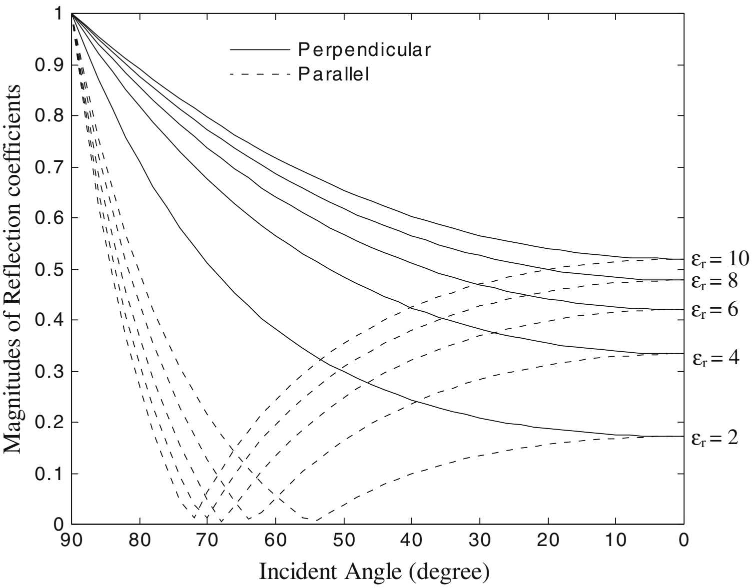

Fig. 2.3 Magnitudes of reflection coefficients of a plane wave incident on different dielectric materials from air

The reflection and transmission coefficients for normal incidence can be obtained from (2.23) to (2.26) by letting $\phi_i = 0$. For instance, the reflection coefficient for the parallel-polarization case is

$$\Gamma_{par} = \frac{\eta_2 - \eta_1}{\eta_2 + \eta_1} \tag{2.29}$$

For low loss and non-magnetic materials, such as those for pavements used in Table 2.1, the intrinsic impedance is almost real and hence can be approximated as $\eta = \sqrt{\mu_o/\varepsilon_o\varepsilon_r} = 377/\sqrt{\varepsilon_r}$ Ohms. Consequently, (2.29) can be rewritten as

$$\Gamma_{par} = \frac{\sqrt{\varepsilon_{r1}} - \sqrt{\varepsilon_{r2}}}{\sqrt{\varepsilon_{r1}} + \sqrt{\varepsilon_{r2}}} \tag{2.30}$$

where ε_{r1} and ε_{r2} are the real parts of the relative dielectric constants of media 1 and 2, respectively.

To verify possible use of (2.30) for practical pavement materials as shown in Table 2.1, the reflection coefficients at the interface between the asphaltand base layers are calculated using (2.29) and (2.30) as a function of the imaginary part of the relative permittivity of the base layer from 0.2 to 0.8 as shown in Table 2.1. As seen in Fig. 2.4, the reflection coefficient calculated from the approximate equation (2.30), assuming lossless materials, shows at most a 1 % difference from those determined from (2.29). Therefore, the assumption of lossless material is reasonable for calculating the reflection coefficients for the considered pavement materials. Similarly, the transmission coefficients can also be calculated for the considered pavement materials assuming lossless materials.

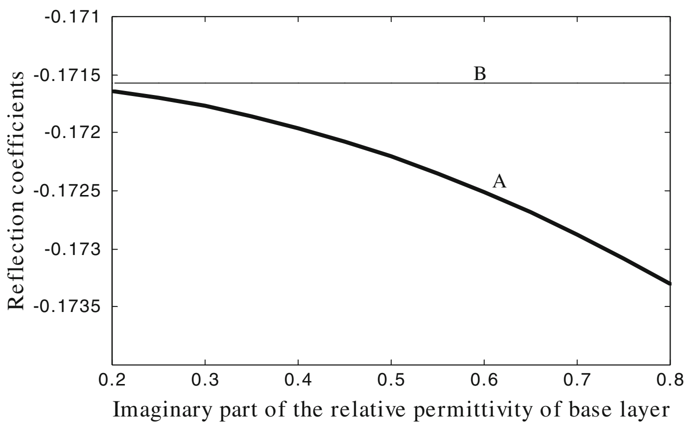

Fig. 2.4 Reflection coefficients A and B for normal incidence at the interface between asphalt and base calculated from (2.28) and (2.29), respectively

From (2.29) or (2.30), the phase of the reflection coefficient is either 0 or π radians. For instance, if the signal is incident from a material with lower dielectric constant to another with higher dielectric constant, the polarity of the reflected signal is opposite to that of the incident signal. This happens with most practical operations of subsurface-sensing radar sensors, such as those for used for assessment of pavements or detection of buried objects. On the contrary, when the incident signal propagates from a material with higher dielectric constant to one having lower dielectric constant, the reflected signal has the same polarity as the incident signal. The polarity of the reflected signal relative to that of the incident signal could be used to aid the analysis of a detected target. For instance, the identical polarity of the reflected signal as compared to the incident signal and the result can be used to detect an air void, which might indicate a defect in pavements, bridges, woods, walls, etc.

For highly lossy materials, where the lossless condition cannot be assumed, the resulting reflection coefficient is not close to real values. The complex reflection coefficient makes the phase of the reflected signal fall between 0 and 2π radians, depending on the losses of the materials. In addition, since the relative dielectric constant is a function of frequency, the phase of the reflection coefficient also changes with the frequency of the incident signal. Therefore, the relative dielectric constants of materials over the frequencies of interest are needed to determine the phases of the reflection coefficients.

2.3.1.2 Reflection and Transmission in Multi-layer Structures

The operations of radar sensors for sensing, particularly subsurface sensing such as pavement characterization, involve structures consisting of multiple layers. In order to analyze the signals propagating in involved media for extracting information of targets, the transmitted and reflected signals, and hence the transmission and reflection coefficients, at the interfaces between different layers need to be determined.

When a sign incident upon a multi-layer structure such as that shown in Fig. 2.5, reflection and transmission occur at multiple interfaces, causing reflected and transmitted signals propagating in these layers. Figure 2.5 illustrates these signals represented by their corresponding electric fields (E's). For simplicity without loss of generality, we only consider three layers and signal reflections up to the third interface. The magnitude of the electric field $E_{r,total}$ of the total reflected signal at the 1st interface, which consists of all the reflected signals, can be expressed approximately as the summation of all the electric fields of the individual reflected signals as

$$E_{r,total} = E_{r1} + E_{r2} + E_{r3} + E'_{r2} \tag{2.31}$$

where E_{r1} is the magnitude of the first reflected electric field at the first interface, E_{r2} is the magnitude of the transmitted electric field through the first interface from

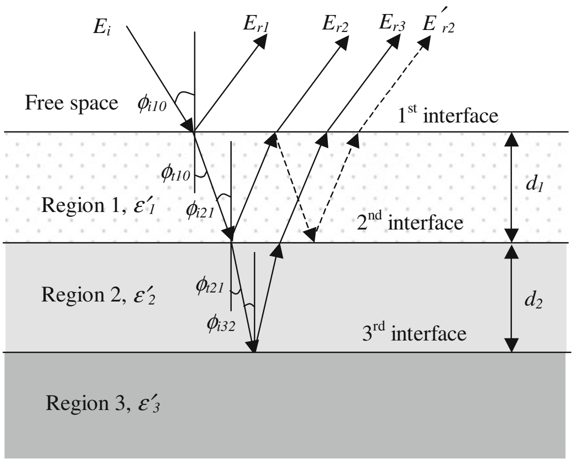

Fig. 2.5 Reflected and transmitted waves in a three-layer structure

the reflected signal at the second interface, E_{r3} is the magnitude of the transmitted electric field through the first interface from the reflected signal at the third interface, and E'_{r2} is the magnitude of the transmitted electric field through the first interface from another reflected signal at the second interface. E_{r1}, E_{r2} and E_{r3} are caused by a single reflection, corresponding to a single-reflected signal, and E'_{r2} is produced by double reflections, corresponding to a double-reflected signal, as can be seen in Fig. 2.5. These electric fields can be expressed as

$$E_{r1} = \Gamma_{10} E_i \tag{2.32}$$

$$E_{r2} = \mathrm{T}_{10}\Gamma_{21}\mathrm{T}_{01}E_i \exp\left(-\frac{2\alpha_1 d_1}{\cos\phi_{t10}}\right)E_i \tag{2.33}$$

$$E_{r3} = \mathrm{T}_{10}\mathrm{T}_{21}\Gamma_{32}\mathrm{T}_{12}\mathrm{T}_{01} \exp\left(-\frac{2\alpha_1 d_1}{\cos\phi_{t10}}\right)\exp\left(-\frac{2\alpha_2 d_2}{\cos\phi_{t21}}\right)E_i \tag{2.34}$$

$$E'_{r2} = \mathrm{T}_{10}\Gamma_{21}\Gamma_{01}\Gamma_{21}\mathrm{T}_{01} \exp\left(-\frac{\alpha_1 d_1}{\cos\phi_{t10}}\right)E_i \tag{2.35}$$

where Γ_{10} and T_{10} are the reflection and transmission coefficients of the signal incident from region 0 to region 1, respectively, ϕ_{t10} indicates the transmitted angle of the signal incident from region 0 to region 1, α_1 and α_2 are the attenuation constants of mediums 1 and 2, respectively, and d_1 and d_2 are the thicknesses of mediums 1 and 2, respectively. The single-reflected electric field magnitude E_{rn} at interface n and the double-reflected electric field magnitude in region n can be generalized, respectively, as

$$E_{rn} = \Gamma_{nn-1}\left[\prod_{m=1}^{n-1} \mathrm{T}_{mm-1}\mathrm{T}_{m-1m} \exp\left(-\frac{2\alpha_m d_m}{\cos\varphi_{tmm-1}}\right)\right]E_i \tag{2.36}$$

$$E'_{rn} = \Gamma^2_{nn-1}\Gamma_{n-2n-1} \exp\left(-\frac{2\alpha_n d_n}{\cos\varphi_{tnn-1}}\right)\left[\prod_{m=1}^{n-1} \mathrm{T}_{mm-1}\mathrm{T}_{m-1m}\right]E_i \tag{2.37}$$

where n and m indicate individual interface or region. In practice, the reflection coefficients are typically smaller than their transmission counterparts, making possible to ignore the double-reflected electric field in the total reflected electric field.

If the incident signal is normal to the structure, the time-average power density $S_{rn}(R)$ reflected from the nth interface can be found as

$$S_{rn}(R) = \Gamma^2_{nn-1}\left[\prod_{m=1}^{n-1} T^1_{mm-1}T^2_{m-1m}\right]\left[\prod_{k=1}^{n-1} \exp(-4\alpha_k d_k)\right]S_i(R) \tag{2.38}$$

where $S_i(R)$ is the time-average incident power density at R, α_k is the attenuation constant of the kth medium, and R is the distance from the interface. Equation (2.36) shows that the reflected power or returned power to the radar sensor will be significantly decreased if the transmission coefficients are small, as expected.

The phase of the transmitted signal propagating through an interface between two different materials, relative to that of the signal incident upon the interface, is determined by the phase of the transmission coefficient. As expressed in Eqs. (2.25) and (2.26), the magnitude of the transmission coefficient is real and positive, and the phase of the transmission coefficient can be between 0 and 2π radians. For lossless materials, especially, the transmission coefficient is a real value, which results in the transmitted signal having the same polarity as the incident signal. Note that the phase of the transmission coefficient depends upon the frequency of the incident signal as well as the losses of the materials.

2.3.2 Radar Cross Section

Radar Cross Section (RCS) of a target, which represents the back-scattering cross section of the target seen by a radar system (and hence is also named "backscatter cross section"), is an important parameter in the design and performance of radar sensors. The RCS mainly depends on the operating wavelength and angle from which the target is viewed by the system, and may be calculated or measured. The RCS is defined as the effective area of the target that intercepts the transmitted power and uniformly (or isotropically) radiates (scatters) all of the incident power in all directions [32]. It can be expressed as

Table 2.2 Radar cross sections of typical geometric shapes. λ is the wavelength

Geometric shapes	Dimension	RCS (σ)
Sphere	Radius r	πr^2
Flat plate	r × r	$4\pi r^2/\lambda^2$
Cylinder	H × radius r	$2\pi r H^2/\lambda$

$$\sigma = 4\pi \frac{\text{time-average scattered power at target toward receiver per unit solid angle}}{\text{time-average power density of incident wave at target}} \tag{2.39}$$

which is mathematically equivalent to

$$\sigma = \lim_{R\to\infty} 4\pi R^2 \frac{\left|\vec{E}_s\right|^2}{\left|\vec{E}_i\right|^2} = \lim_{R\to\infty} 4\pi R^2 \frac{P_s}{P_i} \tag{2.40}$$

where $\vec{E}_s$ and P_s are the scattered electric field and time-average power density magnitude at a distance R away from the target, respectively, $\vec{E}_i$ and P_i are the incident electric field and time-average incident power density magnitude at the target, respectively, and R is the distance between the target and receiving antenna (or the range). It can be inferred from (2.40) that the RCS is independent with R due to the fact that the power density is inversely proportional to R^2; this is expected since the RCS is a property of the target itself. The RCS provides system designers some crucial characteristics of targets observed by radar systems. When the range R is large with respect to wavelength, the incident signal is considered as a uniform plane wave.

Table 2.2 shows the theoretical RCS values of typical geometric shapes in optical regions (i.e., $2\pi r/\lambda > 10$) [23], where the ratio of the calculated RCS to the real cross sectional area of a sphere is 1. These values are very accurate as the RCS of a sphere is independent of the frequency in the optical region. The most typical geometry is a half-space for radar sensors used for surface or subsurface sensing involving structures of multiple media such as pavements consisting of asphalt, base and various subgrade layers, or walls in buildings. The half-space is considered to be an infinite plate that can be either smooth or rough according to the roughness of that plate [31].

2.4 System Equations

2.4.1 Friis Transmission Equation

Friis transmission equation, providing a very simple estimate of the received power with respect to the transmitted power for a general RF system, is a basic equation

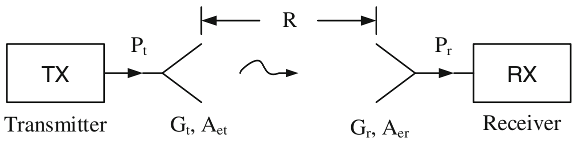

Fig. 2.6 Simple RF system's block diagram. P_t is the output power of the transmitter (TX), which is assumed to be equal to the power transmitted by the transmit antenna. P_r is the power arriving at receiver (RX), which is assumed to be equal to the power received by the receive antenna. G_t, A_{et} and G_r, A_{er} are the gain and effective antenna aperture of the transmit and receive antennas, respectively. R is the distance between the transmit and receive antennas

for communications and sensing. Figure 2.6 shows a simple (bi-static) RF system consisting of transmitter, receiver and antennas. For simplified illustration without loss of generality, we assume that the system and the transmission media are ideal—in which, the system has matched polarization; the antennas, transmitter and receiver are perfectly matched; the antennas are lossless; there is no scattering in signal's transmission and reception; and the antennas and transmission media are lossless.

The effective antenna area or aperture, which specifies the area of antenna that captures incoming energy, is defined as the ratio between the power received by the antenna and its power density. Mathematically, it can be derived as

$$A_e(\theta,\phi) = \frac{\lambda^2}{4\pi} G(\theta,\phi) \tag{2.41}$$

where θ and ϕ are the (angle) coordinates in a spherical coordinate system, λ is the operating wavelength, and $G(\theta,\phi)$ is the gain of the antennaAssume the transmit antenna is isotropic, the power density at the receive antenna, produced by the power illuminating from the transmit antenna, is given as

$$S_r = \frac{P_t}{4\pi R^2} \tag{2.42}$$

The receiving power density corresponding to a transmit antenna having gain G_t, is

$$S_r = \frac{P_t G_t}{4\pi R^2} \tag{2.43}$$

The power received by the receiver is given as

$$P_r = S_r A_{er} = \frac{P_t G_t}{4\pi R^2} A_{er} \tag{2.44}$$

We can derive, upon using (2.41) and (2.44),

$$\frac{P_r}{P_t} = G_t G_r \left(\frac{\lambda}{4\pi d}\right)^2 \tag{2.45}$$

which is known as the *Friis* transmission equation, which gives the optimum received power from a given transmitted power.

In practice, losses occur in system operations due to various reasons such as polarization mismatch between the transmit and receive antennas, scattering, mismatch loss at the transmitter and receiver, and loss in antennas and in the transmission medium. Taking these losses into account yields

$$\frac{P_r}{P_t} = G_t G_r L \left(\frac{\lambda}{4\pi R}\right)^2 \tag{2.46}$$

where $L < 1$ represents the total loss encountered by the system during operation including the system loss itself and loss of the propagating medium. The medium loss is accounted for by the loss factor $\mathrm{e}^{-2\alpha R}$ for power, where α represents the attenuation constant of the medium.

The maximum range of detection or communication corresponds to the received power equal to the minimum power $P_{r,min}$, that can detected by the receiver, and can be determined from (2.46) as

$$R_{\max} = \frac{\lambda}{4\pi}\sqrt{G_t G_r L \frac{P_t}{P_{r,\min}}} \tag{2.47}$$

As can be seen, in order to double the range, the transmitting power must be increased four times, which is substantial.

2.4.2 Radar Equation

Radar equation governs the relationship between the transmitted and received power in radar systems, taking into account the systems' antenna gains, losses, operating frequencies, and ranges and radar cross sections of targets. It is an important equation used in the design and analysis of radar systems.

We consider a monostatic system using two separate antennas co-located or same antenna for transmitting and receiving, as shown in Fig. 2.7. The power density at the target is the same as that given in (2.43) with R denoting the distance from the antennas to the target as seen in Fig. 2.7. The power transmitted by the transmit antenna is intercepted and reradiated (scattered and reflected) by the target in different directions depending on the target's scattering characteristics. In the direction of the receive antenna, considering Fig. 2.7a, the reradiated power is derived as

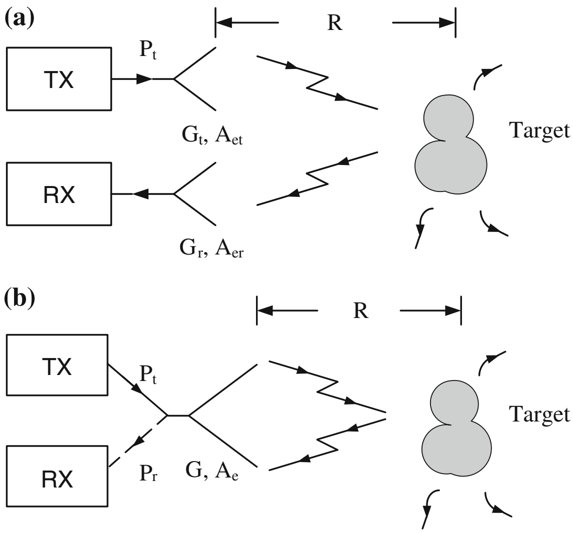

Fig. 2.7 A simple monostatic system with two antennas (**a**) and single antenna (**b**)

$$P_\sigma = \frac{P_t G_t}{4\pi R^2}\sigma \tag{2.48}$$

The power density at the receive antenna due to the power return from the target can be derived, under ideal conditions without any loss, as

$$S_r = \frac{P_t G_t \sigma}{(4\pi R)^2} \tag{2.49}$$

Using the antenna effective area as given in (2.41), the ratio between the power of the target's reflected signal received at the receiver and the power transmitted by the transmitter can be derived as

$$\frac{P_r}{P_t} = \sigma \frac{G_t G_r \lambda^2}{(4\pi)^3 R^4} \tag{2.50}$$

which is commonly known as the radar equation.

For practical systems operating under real conditions, the radar equation becomes

$$\frac{P_r}{P_t} = \sigma \frac{G_t G_r \lambda^2 L}{(4\pi)^3 R^4} \tag{2.51}$$

where $L < 1$ is again the total loss of the system under operation including the system loss and medium loss. The medium loss due to the propagating medium is

$e^{-4\alpha R}$ accounting for the propagation over twice of the target's range. The radar equation in (2.51) can be rewritten imposing this loss into it as

$$\frac{P_r}{P_t} = \sigma \frac{G_t G_r \lambda^2 L' e^{-4\alpha R}}{(4\pi)^3 R^4} \tag{2.52}$$

where L' represents the loss of the system itself. The radar equation involves the transmitted power, antenna gains, system loss and operating frequency, which are controlled and set by the system designer, and the target's RCS maximum range or penetration depth, and attenuation constant of the propagating medium, which, however, are not controlled by the system designer.

The maximum range can be determined from (2.51) and (2.52) as

$$R_{\max} = \left[\frac{P_t \sigma G_t G_r L \lambda^2}{(4\pi)^3 P_{r,\min}}\right]^{1/4} = e^{-\alpha R_{\max}} \left[\frac{P_t \sigma G_t G_r L' \lambda^2}{(4\pi)^3 P_{r,\min}}\right]^{1/4} \tag{2.53}$$

which is proportional to $P_t^{1/4}$. Note that the second expression for R_{max} in (2.53) represents a transcendental equation, which could be solved using a numerical method such as the Newton-Raphson method.

We can now see that, in order to double the maximum range, the transmit power needs to be increased by 16 times, which is very substantial and may not be achievable at RF frequencies for high-power and long-range applications using certain device technologies, particularly in the millimeter-wave regime. Equations (2.51) and (2.52) suggest that larger target's RCS leads to easier detection. As can be recognized by now, the RCS of objects, such as air planes or buried pipes, is a very important parameter to be considered in the design of objects and systems used to detect these objects.

When the transmit and receive antennas in Fig. 2.7a are the same, or considering a single antenna as shown in Fig. 2.7b, the radar equation becomes

$$\frac{P_r}{P_t} = \sigma \frac{G^2 \lambda^2 L}{(4\pi)^3 R^4} = \sigma \frac{G^2 \lambda^2 L' e^{-4\alpha R}}{(4\pi)^3 R^4} \tag{2.54}$$

where $G = G_t = G_r$ is the antenna gain, and the corresponding maximum range is

$$R_{\max} = \left[\frac{P_t \sigma L G^2 \lambda^2}{(4\pi)^3 P_{r,\min}}\right]^{1/4} = e^{-\alpha R_{\max}} \left[\frac{P_t \sigma L' G^2 \lambda^2}{(4\pi)^3 P_{r,\min}}\right]^{1/4} \tag{2.55}$$

Making use of (2.21), the squared magnitude of the incident field E_i, where $|E_i| = |E_0| e^{-\alpha R}$ with E_o being the initial amplitude of the transmitted electric field at the antenna, at the target can be obtained for a single-antenna monostatic system, as shown in Fig. 2.7b, as

$$|E_i|^2 = \frac{|2\eta|}{\cos\phi_\eta} \frac{P_t G e^{-2\alpha R}}{4\pi R^2} \tag{2.56}$$

The signal scattered from the target is attenuated as it propagates toward the antenna, and the squared magnitude of the scattered field E_s at the antenna can be derived as

$$|E_s|^2 = \frac{|2\eta|}{\cos\phi_\eta} \frac{P_r'}{A_e} \tag{2.57}$$

where $P_r' = P_r/G$ is the power captured by the antenna.

2.5 Signal-to-Noise Ratio of Systems

In practical operations, system's performance is affected by noise. Noise affecting a system operation can be classified into two kinds: external noise and internal noise. External noise represents noise caused by the environment surrounding the system, including noise injected from nearby stationary and moving objects. This noise is typically large at low frequencies but small in the RF range and is, in general, negligible as compared to the internal noise generated by the RF receiver itself. Receiver noise is the dominant noise in a system and is inherent in the receiver. In operation, the output signal of the receiver includes signals produced by desired targets as well as those from clutters, external noise and interference. Figure 2.8 shows a sketch of output voltage of a receiver. If the noise level contributed by the receiver itself is high or the received signal is weak, the system cannot perform accurately its intended function such as detecting a target. Typically, a threshold

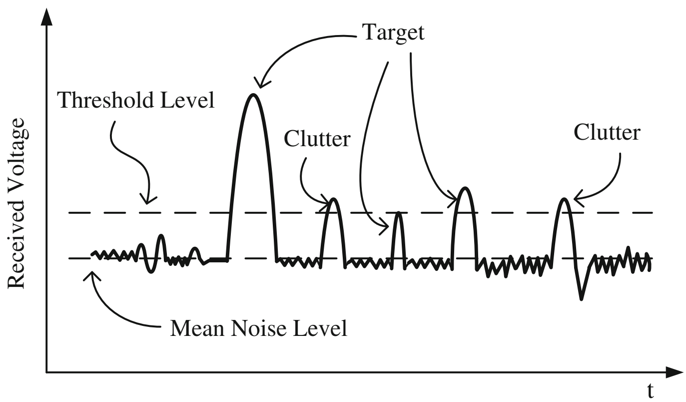

Fig. 2.8 Output voltage of a receiver

level is used to reduce the noise and clutter effects. However, if the threshold level is set to be sufficiently high, it will reduce the sensing capability of the system. For low threshold levels, on the other hand, inaccurate detection may result. Clutter effects can be reduced and identified by signal processing techniques. To increase the sensing capability or to enhance the communication performance of a system, the receiver's noise needs to be reduced or, equivalently, the receiver's signal-to-noise ratio (S/N) needs to be increased. This noise, although unavoidable, can be controlled to some extent by RF designers.

Receiver noise is, in general, contributed by three different noises. One is conversion noise generated during certain receiver operation—for example, FM-AM conversion noise. The other noise is low-frequency noise generated in the mixing process. The conversion and low-frequency noises depend on the receiver type—for instance, homodyne or FMCW receiver. The third noise contribution is thermal or Johnson noise generated by thermal motion of electrons in receiver's components. This noise always exists in receivers. We consider only thermal noise here.

The maximum thermal noise power available at the receiver's input is given as

$$P_{Ni} = kTB \tag{2.58}$$

where $k = 1.374 \times 10^{-23}$ J/K is the Boltzmann's constant, T is the temperature in Kelvin degree (K) at the receiver's input, and B is the noise bandwidth in Hertz (Hz), which is the absolute RF bandwidth over which the receiver operates. The available noise power P_{Ni} is independent of the receiver's operating frequency. In typically operating room temperature (62 °F), the thermal noise (kT) is about −174 dBm/Hz. As can be seen, this noise can be sufficiently large over a large bandwidth that degrades the noise performance of receiver and hence system substantially.

We define an ideal or noiseless receiver as a receiver that adds no additional noise as the input thermal noise P_{Ni} passes through it, except increasing the thermal noise level by the gain of the receiver. We now consider an actual (non-ideal) receiver that adds extra noise to that produced by an ideal receiver and define the noise figure of such receiver as

$$F = \frac{\textit{output noise power of actual receiver}}{\textit{output noise power of ideal receiver}} \frac{P_{No}}{GP_{Ni}} = \frac{P_{No}}{kTBG} \tag{2.59}$$

where G is the available power gain of the receiver defined as

$$G = \frac{P_{So}}{P_{Si}} \tag{2.60}$$

with P_{Si} and P_{So} being the (real) signal's available power at the input and output of the receiver, respectively. The total noise power at the output of the receiver can then be obtained as

$$P_{No} = FkTBG = kT_nBG \tag{2.61}$$

where $T_n \equiv FT$, the thermal noise power per Hz, is defined as the (equivalent) "noise temperature" of the receiver. The noise figure of receivers can be obtained from (2.59) and (2.61) as the ratio between the input *S/N* and output *S/N* of receivers:

$$F = \frac{P_{Si}/P_{Ni}}{P_{So}/P_{No}} = \frac{\textit{signal-to-noise ratio at input}}{\textit{signal-to-noise ratio at output}} \tag{2.62}$$

which is more commonly known to RF engineers than (2.59). As can be seen, the noise figure indeed reduces the output S/N level of the receiver used in subsequent processing for sensing or communication purposes. This receiver's figure of merit contributes to the overall receiver's noise and is considered as one of the most important parameters of the receiver. In the design of receivers, it is important to minimize the noise figures of individual components, particularly those close to front of the receivers. A typical receiver consists of cascade of components—for example, a super-heterodyne receiver front-end primarily comprising of band-pass filter, low-noise amplifier, mixer and IF amplifier—and its noise figure depends on the receiver's individual components. It is noted that the noise figure of a passive component such as band-pass filter is equal to the reciprocal of the insertion loss of that component. For instance, a band-pass filter with a −3-dB insertion loss would have a noise figure equal to 2 or, in term of decibel, 3 dB. The (output) *S/N* of the receiver, making use of the radar equation (2.52), can be derived as

$$\frac{S}{N} = \sigma \frac{P_t G_t G_r \lambda^2 L' e^{-4\alpha R}}{(4\pi)^3 R^4 FkTB} \tag{2.63}$$

It is particularly noted that in actual system operations, the *S/N* value produced by receivers is much more important than the absolute powers of real and noise signals received by receivers.

2.6 Receiver Sensitivity

Receiver sensitivity indicates the minimum detectable input signal level for a receiver and hence measures the ability of a receiver to detect a signal. A system can detect a signal returned from a target or sent by another system if the received power is higher than the receiver sensitivity. The receiver sensitivity (*SR*) is determined by the noise temperature (*Tn*), bandwidth (*B*), noise figure (*F*), and signal-to-noise ratio (*S/N*) of the receiver.

Figure 2.9 depicts the sensitivity required for a receiver to detect a returned signal. The noise temperature (*kT*) entering the receiver is increased over the

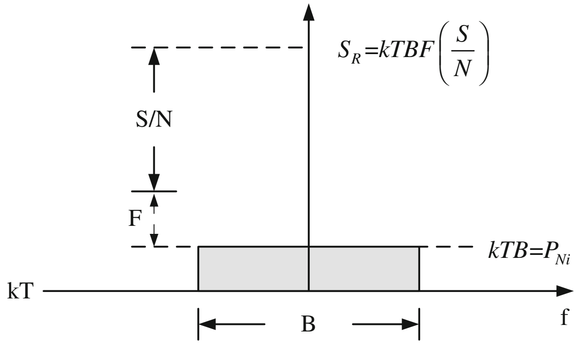

Fig. 2.9 Sensitivity of a receiver. $P_{Ni} = kTB$ is the input noise power

receiver's bandwidth to kTB, which is then further expanded through the noise figure and S/N of the receiver to reach a value of $kTBF(S/N)$. This final noise level is defined as the sensitivity of the receiver or the minimum input signal power that can be detected by the receiver:

$$S_R = kTBF\left(\frac{S}{N}\right) \tag{2.64}$$

Note that S_R is not the power density. The maximum range of a systems, achieved when the received power is equal to the receiver sensitivity, can be rewritten using (2.51) or (2.52) and (2.63) as

$$R_{\max} = \left[\frac{P_t\sigma G_t G_r L\lambda^2}{(4\pi)^3 kTBF\left(\frac{S}{N}\right)}\right]^{1/4} = \mathrm{e}^{-\alpha R_{\max}}\left[\frac{P_t\sigma G_t G_r L'\lambda^2}{(4\pi)^3 kTBF\left(\frac{S}{N}\right)}\right]^{1/4} \tag{2.65}$$

A remark needs to be mentioned here concerning the average and peak powers. It is useful to consider the average power such as the average transmitting power, which is given as

$$P_{t,avg} = \frac{P_t}{B} \tag{2.66}$$

where B is the absolute (RF) bandwidth of the transmitter and receiver, in evaluating the system's parameter such as the maximum range. The average transmitting power is one of the controllable factors extensively used in designing a system and relates to the type of the waveform used. Using the average transmitting power, we can rewrite (2.65) as

$$R_{\max} = \left[\frac{P_{t,avg}\sigma G_t G_r L\lambda^2}{(4\pi)^3 kTF\left(\frac{S}{N}\right)}\right]^{1/4} = \mathrm{e}^{-\alpha R_{\max}}\left[\frac{P_{t,avg}\sigma G_t G_r L'\lambda^2}{(4\pi)^3 kTF\left(\frac{S}{N}\right)}\right]^{1/4} \tag{2.67}$$

It can be deduced from (2.67) that high average transmitting power combined with less bandwidth results in long range or deep penetration.

2.7 Performance Factor of Radar Systems

The system performance factor (SF) of a system can be defined as [33]

$$SF = \frac{P_t}{S_R} \tag{2.68}$$

This factor is the system's figure of merit used to measure the overall performance of a system and is one of the most important parameters in the system equation for estimating the system's range. As the minimum detectable signal corresponds to the maximum range of a system, we can derive the system performance factor, utilizing (2.51) or (2.52), (2.64) and (2.68), by letting the received power equal to the receiver sensitivity (S_R) as

$$SF = \frac{(4\pi)^3 R_{\max}^4}{G_t G_r L \sigma \lambda^2} = \frac{(4\pi)^3 R_{\max}^4}{G_t G_r L' \sigma \lambda^2 \mathrm{e}^{-4\alpha R_{\max}}} \tag{2.69}$$

The performance factor given in (2.69) neglects the contribution of the receiver. In practical systems, however, the system performance factor is limited by the actual receiver dynamic range. Hence, it is necessary to incorporate a correction for the receiver dynamic range into the system performance factor as we will address in the analysis of SFCW radar sensor in Chap. 3.

2.8 Radar Equation and System Performance Factor for Targets Involving Half-Spaces

The radar equations described in Sect. 2.5 are general radar equations. To provide more details and insight for specific applications such as those involving sensing of multi-layer structures like pavements or buried objects, the radar equation needs to be modified taking into account the specific conditions encountered in such applications to enable more accurate characterization such as estimation of maximum range or penetration depth.

We first consider a single half-space target spaced at a distance R from an antenna as shown in Fig. 2.10a and assume a uniform plane wave incident normal to the interface. Following the derivation of (2.44), we can derive the power received by the antenna, considering the reflection at the interface, the roundtrip travel of $2R$, and the loss of the propagating medium, as

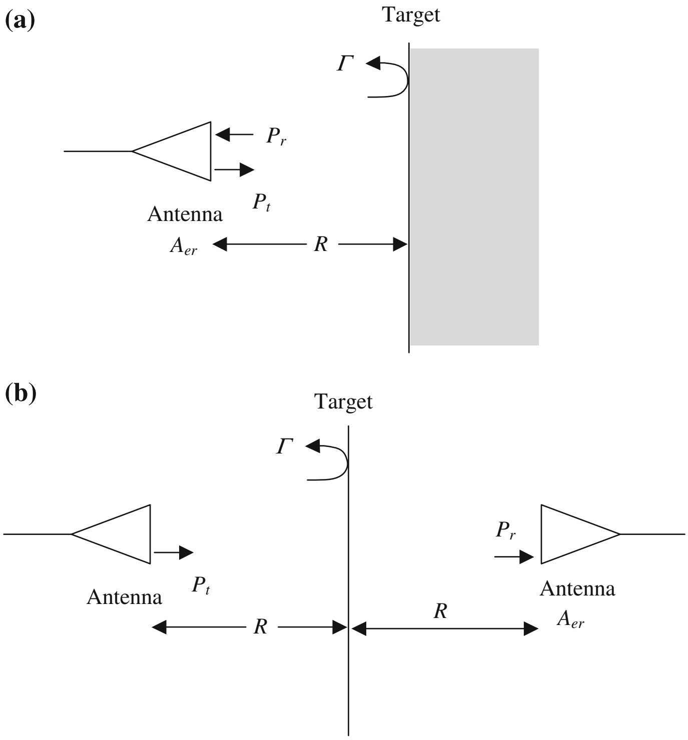

Fig. 2.10 Single half-space target illuminated with a uniform plane wave from an antenna (**a**) and its equivalent using the image technique (**b**)

$$P_r = \frac{P_t G_t A_{er} L}{4\pi (2R)^2} \Gamma^2 \tag{2.70}$$

where Γ is the magnitude of the reflection coefficient and L (<1) is the loss of the medium. The *RCS* of a half-space is found from (2.51) utilizing (2.41) and (2.70) as

$$\sigma = \pi R^2 \Gamma^2 \tag{2.71}$$

Equation (2.39) can also be derived considering Fig. 2.10b obtained by applying the image technique presented in [31].

We now consider a target consisting of two layers with each layer assumed to be a half-space to exemplify the analysis of a more general multi-layer target. This simple structure simplifies the formulation and show signal interactions without loss of generality. Figure 2.11a shows a two-layer half-space target with a uniform plane wave traveling obliquely to the first interface and the antennas with the same gain are located next to each other. Extending the foregoing analysis for a single interface to two consecutive interfaces depicted in Fig. 2.11a or analyzing the

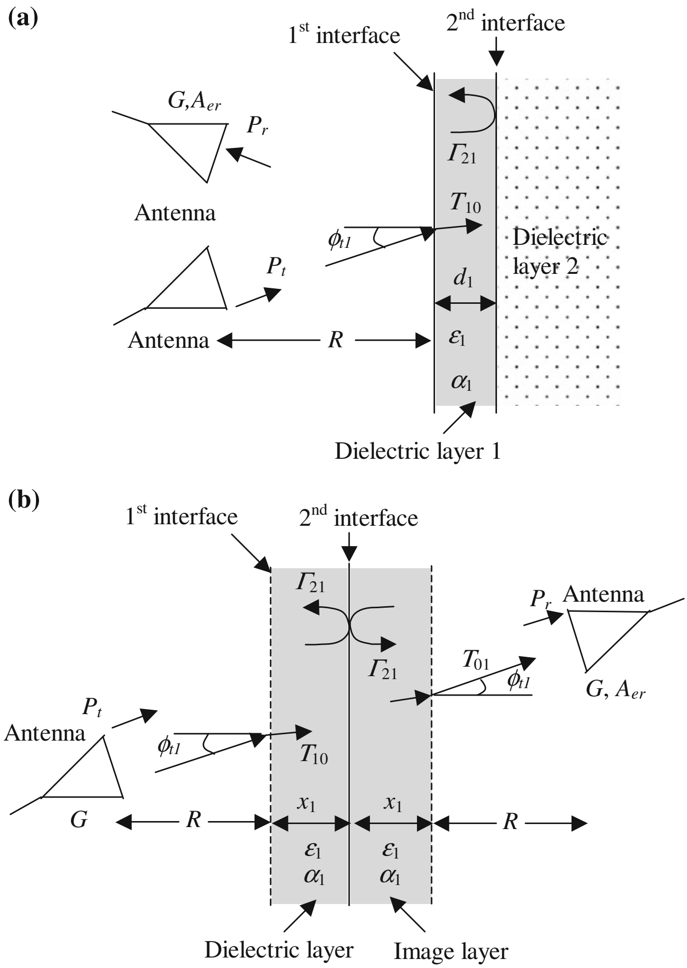

Fig. 2.11 Two-layer half-space target illuminated with a uniform plane wave (**a**) and its equivalent using the image technique (**b**)

equivalent structure shown in Fig. 2.11b obtained by applying the image principle, we can derive the power received by the antenna from (2.70). To that end, we replace the reflection coefficient Γ in (2.70) with the composite reflection coefficient upon reflections from the two interfaces from (2.33) as

$$\Gamma = \mathrm{T}_{10}\Gamma_{21}\mathrm{T}_{01}\exp\left(-\frac{2\alpha_1 d_1}{\cos\phi_{t10}}\right) \tag{2.72}$$

and the distance R in Eq. (2.70) with, considering the oblique incidence,

$$R = \frac{R}{\cos\phi_{i1}} + \frac{x_1}{\cos\phi_{t10}} \quad (2.73)$$

where ϕ_{i1} and ϕ_{t10} are the incident and transmitted angles at the first interface, respectively. Note that the thickness of layer 1, d_1, should be replaced with $x_1 = d_1\sqrt{\varepsilon_{r1}}$, where ε_{r1} is the relative dielectric constant of layer 1, as the signal's velocity is reduced in the layer. The radar equation, which determines the power received at the antenna upon reflection from the second interface, can now be expressed as

$$P_{r2} = \frac{P_t G^2 \lambda^2 L}{(4\pi)^2 \left(\frac{2R}{\cos\phi_{i1}} + \frac{2x_1}{\cos\phi_{t10}}\right)^2} \Gamma_{21}^2 \mathrm{T}_{10}^2 \mathrm{T}_{01}^2 \exp\left(-\frac{4\alpha_1 d_1}{\cos\phi_{t10}}\right) \quad (2.74)$$

The result in (2.74) can be generalized to obtain the radar equation for multi-layer targets with each layer assumed to be a half-space as

$$P_{rn} = \frac{P_t G^2 \lambda^2 L \Gamma_{nn-1}^2 \left[\prod_{m=1}^{n-1} \mathrm{T}_{mm-1}^2 \mathrm{T}_{m-1m}^2 \exp\left(\frac{-4\alpha_m d_m}{\cos\phi_{tmm-1}}\right)\right]}{(4\pi)^2 \left(\frac{2R}{\cos\phi_{i1}} + \sum_{l=1}^{n-1} \frac{2x_l}{\cos\phi_{tll-1}}\right)^2} \quad (2.75)$$

where P_{rn} is the power arriving at the receive antenna from the nth interface.

The nth interface is detectable if $P_{rn} \geq S_R$. Consequently, the radar's system performance factor SF is found using (2.68), (2.69) and (2.75) as

$$SF = \frac{64\pi^2 \left(\frac{R}{\cos\phi_{i1}} + \sum_{l=1}^{n-1} \frac{x_l}{\cos\phi_{tll-1}}\right)^2}{G^2 \lambda^2 L' \Gamma_{nn-1}^2 \left[\prod_{m=1}^{n-1} \mathrm{T}_{mm-1}^2 \mathrm{T}_{m-1m}^2 \exp\left(-\frac{4\alpha_m d_m}{\cos\phi_{tmm-1}}\right)\right]} \quad (2.76)$$

Equation (2.76) can be used to estimate the maximum range or penetration depth of radar sensors for sensing multi-layer half-space targets such as pavement layers.

2.9 Radar Equation and System Performance Factor for Buried Objects

Figure 2.12 shows an object buried in a medium underneath a surface, which is illuminated with a uniform plane wave in air (assumed to be lossless) from an antenna. The time-average power density S at the object can be derived from (2.43), taking into account the oblique incidence, transmission coefficient T_{10} at the surface and attenuation constant α_1 of the medium, as

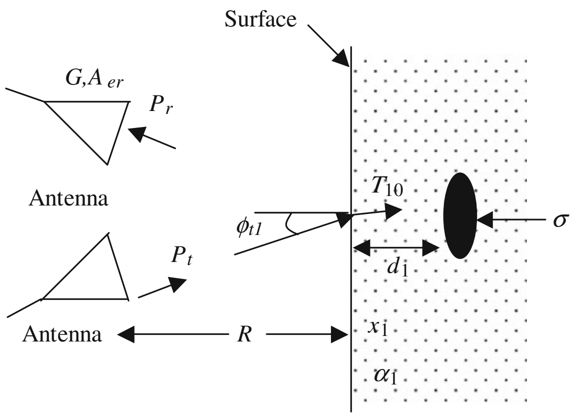

Fig. 2.12 Buried object under a surface

$$S = \frac{P_t G_t}{4\pi\left(\frac{R}{\cos\varphi_{i1}} + \frac{x_1}{\cos\varphi_{t10}}\right)^2} \mathrm{T}_{10}^2 \exp\left(-\frac{2\alpha_1 d_1}{\cos\phi_{t10}}\right) \tag{2.77}$$

The *RCS* of the object is assumed to be approximately equal to that of a half-space as

$$\sigma = \pi\left(\frac{R}{\cos\phi_{i1}} + \frac{x_{1\max}}{\cos\phi_{t10}}\right)^2 \Gamma^2 \tag{2.78}$$

where Γ is the reflection coefficient at the object's surface. The reflected power from the object can then be obtained from (2.74) making use of (2.41) and (2.71) as

$$P_r = \frac{P_t G A_{er} \sigma L'}{(4\pi)^2\left(\frac{R}{\cos\phi_{i1}} + \frac{x_1}{\cos\phi_{t10}}\right)^4} \mathrm{T}_{10}^2 \mathrm{T}_{01}^2 \exp\left(-\frac{4\alpha_1 d_1}{\cos\phi_{t10}}\right) \tag{2.79}$$

Consequently, the system performance factor defined in (2.68) can be derived as

$$SF = \frac{64\pi^3\left(\frac{R}{\cos\phi_{i1}} + \frac{x_{1\max}}{\cos\phi_{t10}}\right)^4}{G^2\lambda^2\sigma \mathrm{T}_{10}^2 \mathrm{T}_{01}^2 L' \exp\left(-\frac{4\alpha_1 d_{1\max}}{\cos\phi_{t10}}\right)} \tag{2.80}$$

where $d_{1\max} = x_{1\max}\big/\sqrt{\varepsilon_{r1}}$, from which the maximum detectable range, d_{1max}, under the surface can be determined.

2.10 Targets Consisting of Multiple Layers and Buried Objects

The analysis becomes more complex for targets involving objects buried within multi-layer structures such as those shown in Fig. 2.13. This target model illustrates some practical targets such as a pavement or wood composite consisting of multiple layers with defects such as voids. Figure 2.13 shows multiple transmissions and reflections, represented by T's and Γ's, respectively, resulted from a signal incident from air upon the surface. Conventional techniques of modeling wave propagation in a multi-layer structure that lead to the radar equations and system performance factors, as described in the foregoing Sects. 2.8 and 2.9, are based on the following assumptions: (1) only a propagating uniform plane wave exists in the entire structure, (2) the layers are homogeneous (e.g., no voids), and (3) reflection coefficient of the final wave reflected off of the surface is the sum of all the reflection coefficients of the individual waves reflected pass the first interface toward the left. These assumptions are not very accurate for structures having objects embedded in multiple layers such as that shown in Fig. 2.13. When a signal is incident this structure at high frequencies, the incident wave will excite an infinite number of different waves, including propagating and evanescent waves, at the first interface. These generated waves are reflected and transmitted into air and the first layer, respectively. Part of the transmitted waves will also produce other reflected and transmitted waves upon incident to the buried objects in the first layer. This process will then continue in subsequent layers. Although the evanescent waves die with distance away from the interfaces and buried objects, their effects would be significant near the interfaces and objects at these frequencies and must be considered for accurate determination of the final reflection coefficient and hence the radar equation and system performance factor. These effects can be considered in the propagation analysis using various full-wave EM techniques such as the mode-matching method [34].

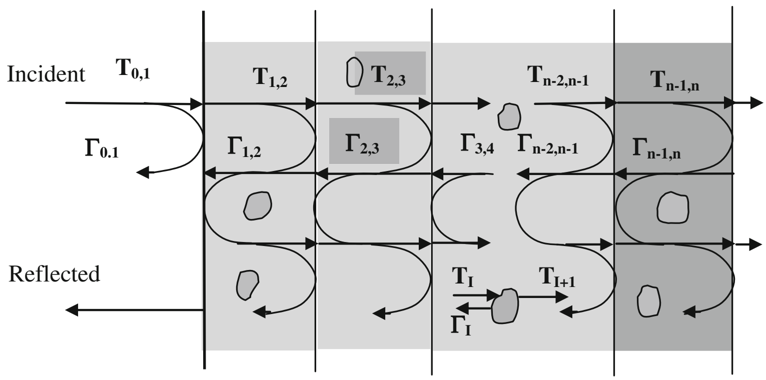

Fig. 2.13 Buried objects within multiple layers

2.11 Summary

This chapter addresses the general analysis of radar sensors. Specifically, it discusses signal propagation in media encountered in using radar sensors, signal scattering from objects, systems equations including Friis transmission equation and radar equations, signal-to-noise ratio, receiver sensitivity, maximum range or penetration depth, and system performance factor. Understanding these basic parameters provides general insight of a radar sensor's possible performance and operation and allows its general analysis to be conducted, which are essential toward the design of microwave systems for sensing applications.

http://www.springer.com/978-3-319-12270-0

Stepped-Frequency Radar Sensors
Theory, Analysis and Design
Nguyen, C.; Park, J.
2016, VIII, 129 p. 81 illus., 80 illus. in color., Softcover
ISBN: 978-3-319-12270-0